

The Society shall not be responsible for statements or opinions advanced in papers or in discussion at meetings of the Society or of its Divisions or Sections, or printed in its publications. Discussion is printed only if the paper is published in an ASME Journal. Released for general publication upon presentation. Full credit should be given to ASME, the Technical Division, and the author(s). Papers are available from ASME for nine months after the meeting.  
Printed in USA.

Copyright © 1983 by ASME

X-RAY TOMOGRAPHY APPLIED TO NDE OF CERAMICS

J. W. Kress and L. A. Feldkamp  
Engineering and Research Staff  
Research  
Ford Motor Company  
Dearborn, Michigan

ABSTRACT

An x-ray radiographic NDE system specifically suited to three-dimensional tomographic reconstruction is described. The results of two applications of the system are discussed. The first is the reconstruction of a section of a ceramic gas turbine rotor blade. This demonstrates the system's ability to reconstruct parts with complex external shape. In the second, an assembly of ceramic components containing a 50  $\mu\text{m}$  gap is examined. The 50  $\mu\text{m}$  gap is detected. This work was supported in part by the Office of Naval Research under contract N00014-78-C-0714.

NOMENCLATURE

$F(x,y,z)$	reconstruction value at the specimen position defined by $x$ , $y$ and $z$
$g(Y)$	horizontal convolution function
$h(Z)$	vertical convolution function
IB	baseline reference image
IO	full intensity reference image
$P_{\alpha}(Y,Z)$	projection function for angle $\alpha$ at detector position defined by $Y$ and $Z$
$Q_{\alpha}(Y,Z)$	convoluted projection function for angle $\alpha$ at detector position defined by $Y$ and $Z$
T	transmission from which projection function is calculated
$x,y,z$	Cartesian coordinates in coordinate system fixed in specimen
$X,Y,Z$	Cartesian coordinates in coordinate system fixed in space and centered at x-ray source
$X_1,Y_1,Z_1$	coordinate of reconstruction position
$X_2,Y_2,Z_2$	coordinate of point on the detector

$X_R$	X coordinate of specimen rotational axis
$\alpha$	rotational angle
$\theta'$	polar angle relative to X axis

INTRODUCTION

It is becoming increasingly clear that ceramics such as silicon nitride will be very important engineering materials in the near future. However, development and practical utilization is crucially dependent on the existence of nondestructive techniques for evaluation of the quality of parts manufactured from these materials. A particular area of concern is the detection and characterization of very small (25 to 50  $\mu\text{m}$ ) fabrication flaws in gas turbine components of complex shape.

X-ray radiography is a technique currently in use for nondestructive evaluation (NDE) of ceramics. Unfortunately, film radiography is not suited to fast, efficient real-time NDE. Real-time x-ray radiography systems consisting of an x-ray source, fluorescent screen or image intensifier, TV camera, monitor, and sample manipulation devices are being developed and marketed and do allow faster inspection. However, their ability to define the location, structure and even (in the case of small flaws) the existence of defects in the sample is limited.

The advent of high-speed/large-memory video (TV) image digitizers with associated minicomputers has made possible the efficient processing of video images as numerical data. Adding this capability to a real-time x-ray radiographic inspection system increases the potential detection capability of the system by permitting accumulation of images in the computer, thereby enabling smaller contrast differences to be seen. Further, the techniques of digital image processing can be applied for additional image enhancement and feature analysis.<sup>(1)</sup>

Unfortunately, a limited number of projection images of the specimen may not be sufficient to characterize small defects, and a large number may overwhelm the observer with information. X-ray tomography

provides a systematic way of organizing large amounts of data into a coherent representation of the internal structure of the sample. This representation is also amenable to many modes of analysis and display.

In x-ray tomography, radiographs of the specimen are taken from many different viewing angles and processed mathematically to yield a numerical representation of the internal density distribution of the sample. All the components needed to perform the tomographic reconstruction are present in a computerized real-time radiographic system. We are developing such a system and are investigating its potential for the detection of small fabrication flaws in ceramic materials.

In the following section the experimental system is described. We then present a brief discussion of the three-dimensional reconstruction algorithm. Results of the application of the tomographic reconstruction procedure to ceramic samples exhibiting features such as complex shape, small defect sizes and complex internal structure are then discussed. Finally, we summarize the results and mention future directions of research to be pursued.

#### EXPERIMENTAL SYSTEM

A block diagram of the tomographic system is given in Fig. 1. The Magnaflux microfocus x-ray tube is

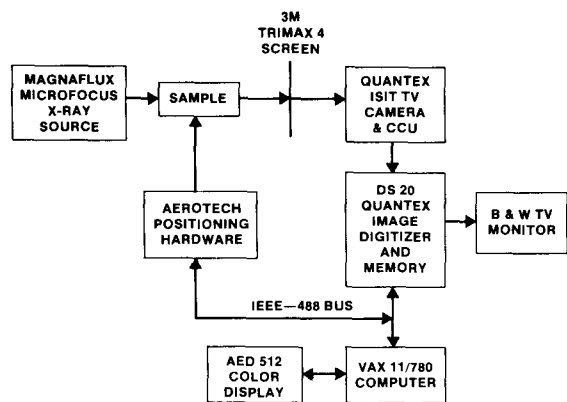


Fig. 1 Block diagram of the tomographic system.

operated to yield a 50  $\mu\text{m}$  source spot size. The specimen is mounted on a small x-ray goniometer for detailed alignment. The goniometer itself sits on Aerotech rotational and translational stages for sample positioning. The 3M Trimax 4 fluorescent screen is imaged by a Quantex ISIT vidicon, which has very high sensitivity and moderate resolution. The Quantex DS-20 performs a 512 x 512 8-bit digitization of the video signal from the camera and then stores (or accumulates) the image in a memory with 12 bits per picture element (pixel). Each pixel is regarded as a detector. The TV monitor is used to observe the live video picture or the

contents of memory. Data transfer from the DS-20 and sample positioning are controlled by the VAX 11/780 via the IEEE-488 bus. Tomographic reconstruction is carried out in the VAX, and additional display and image processing capability is provided by the AED 512 color display terminal.

The system linear resolution function, referenced to the specimen position, is approximately triangular with a full-width at half maximum of 250 to 500  $\mu\text{m}$ , depending on magnification. This represents the combined effects of source spot size, screen resolution, lens distortion, vidicon resolution and digitizer instability. We estimate the limiting resolution to be 25 to 50  $\mu\text{m}$ . By averaging images, using both the DS-20 and the VAX, we can attain a one percent standard deviation in a measurement of specimen transmission.

Data acquisition and reconstruction is completely automated and typically proceeds as follows. A baseline reference image (IB) is accumulated with the x-ray beam blocked with lead. A full intensity reference image (IO) is then taken in an open-screen configuration. The sample is then moved into position and the first sample projection image is taken. As the sample image is accumulated in the VAX, it is corrected for baseline shifts (using IB and a black reference) and for intensity fluctuations (using IB, IO and a strip of pixels which represent unattenuated rays). After image averaging at this position, the transmissions T are calculated on a two-dimensional array of detectors. From this we calculate an array representing the projection function, given in first approximation by  $P = \ln(1/T)$ . The reconstruction algorithm is then applied and the matrix containing the reconstruction is updated. The specimen is rotated and the process is repeated until each angle of a set equally spaced about 360 degrees has been examined, whereupon the result of the reconstruction is stored on disk and is available for examination or further processing.

#### RECONSTRUCTION ALGORITHM

The principal application of computerized tomography (CT) has been in medical systems, where cross sections of the human body are reconstructed from data collected by measurements of the attenuation of x-rays along lines in the desired planes. In these applications two-dimensional images are generated from one-dimensional detector arrays. Data for successive cross sections is acquired by translating the patient along the axis of the scanner. (2)

By contrast, we begin with a two-dimensional detection system. This additional dimension of detection should, in principle, allow a three-dimensional reconstruction of a specimen. This ability to reconstruct the specimen in three dimensions is of considerable importance for NDE since it allows a natural inspection of a significant portion of the specimen while minimizing the mechanical complexity, and hence the cost, of the system.

To take advantage of two-dimensional projection images, we require what is called a 'direct three-dimensional' or 'cone-beam' algorithm. To our knowledge, no commercial CT scanner embodies such an approach. The 'Dynamic Spatial Reconstructor (DSR)', a highly sophisticated system (3) being developed at the Mayo Clinic for temporal studies of the human heart, collects two-dimensional projection data and so requires, in principle, the same sort of algorithm.

However, the small angle subtended by the detector system of the DSR allows it to utilize standard two-dimensional methods with very little error (3). Various direct 3-D methods have been described in the literature [see, for example, papers cited in (4)], but none of these is satisfactory for our application. The algorithm we have developed and are using is described briefly here and will be discussed in detail in a separate report. (5)

We have generalized to three dimensions the type of algorithm used in most commercial CT scanners, a convolute-and-backproject method. The reconstruction process consists of a convolution of geometrically weighted projection data followed by a weighted back-projection, or smearing, of the convoluted data along lines from points in the detector plane back toward the source. In this way, the contributions to the density at a point in the reconstruction space is determined by the convoluted data at the projections of that point.

In Fig. 2 we represent the geometrical arrangement of the tomographic system.

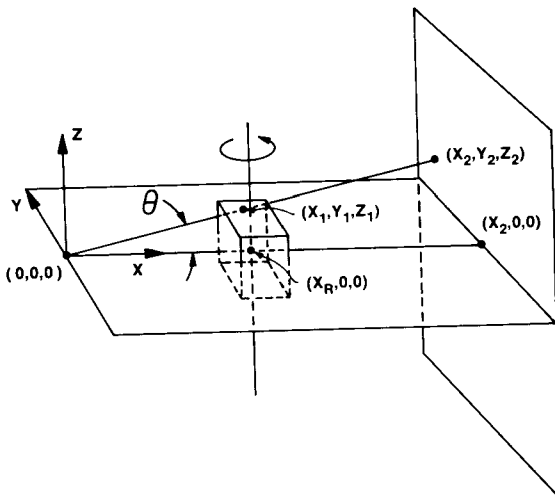


Fig. 2 Geometric arrangement of the tomographic system. For the results cited in this paper  $X_R = 4.57$  cm and  $X_2 = 20.1$  cm.

A coordinate system is fixed in space with center at the x-ray source. A point in this system is denoted by  $(X, Y, Z)$ . The specimen rotates about an axis parallel to the Z direction and passing through the point  $(X_R, 0, 0)$ . The detector array is in an Y-Z plane; points on the detector plane are denoted by  $(X_2, Y_2, Z_2)$ , where  $X_2$  is a constant. A second coordinate system rotates with the specimen and is centered about the point  $(X_R, 0, 0)$ ; in this coordinate system, a position in the specimen may be labelled by  $(x, y, z)$ . If the rotational angle is  $\alpha$ , this point is given by

$$(X_1, Y_1, Z_1) = (X_R + x \cos \alpha + y \sin \alpha, -x \sin \alpha + y \cos \alpha, z) \quad (1)$$

in the fixed system. The projection data for angle  $\alpha$  are denoted by the function  $P_\alpha(Y, Z)$ . From this we

generate the convoluted projection function

$$Q_\alpha(Y, Z) = \iint dY' dZ' \cos \theta' P_\alpha(Y', Z') g(Y - Y') h(Z - Z'), \quad (2)$$

where  $g(Y)$  and  $h(Z)$  are the horizontal and vertical convolution functions, respectively, and  $\cos \theta'$  is a weighting factor, given by

$$\cos \theta' = X_2 / (X_2^2 + Y'^2 + Z'^2)^{1/2}. \quad (3)$$

The reconstruction formula is then

$$F(x, y, z) = (1/4\pi^3) \int d\alpha Q_\alpha(Y_2, Z_2) X_R X_2 / X_1^2. \quad (4)$$

Note that  $(Y_2, Z_2)$  is the detector-plane projection of the reconstruction point  $(X_1, Y_1, Z_1)$ , given in Eq. (1) in terms of  $(x, y, z)$ , i.e.,

$$Y_2 = (X_2/X_1) Y_1 \quad (5)$$

$$Z_2 = (X_2/X_1) Z_1. \quad (6)$$

In practice, the projection function is represented by a discrete sampling, and the integrals in Eqs. (2) and (4) are performed in discrete form. Except in the plane  $Z=0$ , the reconstruction method just summarized is mathematically approximate, even if the data are perfect. The nature of the blurring induced by the method will be discussed in some detail in (5). Here we merely note that the deficiencies of the algorithm are relatively minor in comparison with the resolution and noise limitations of the original data.

## RESULTS

Many ceramic components envisioned for turbine use are of complex shape. NDE of complex shaped objects is difficult using conventional methods, so an early test of the tomographic system was a reconstruction of a specimen with a complex external shape. A section of a single blade removed from a silicon nitride turbine rotor was reconstructed. The results are displayed in Fig. 3 as a cross sectional slice. The airfoil shape is well reproduced.

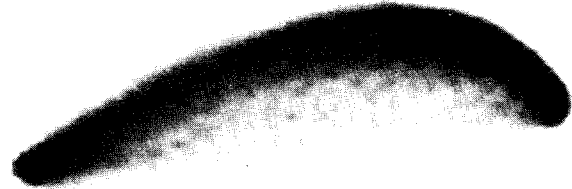


Fig. 3 Result of application of the tomographic reconstruction procedure to a blade from a silicon nitride turbine rotor. The result is displayed as a cross sectional slice.

Another demanding test of an NDE method is the detection and characterization of flaws which are extended in two dimensions but small (25 to 50  $\mu\text{m}$ ) in the remaining dimension. A flaw of this type can be simulated by an assembly of ceramic pieces as shown in Fig. 4.

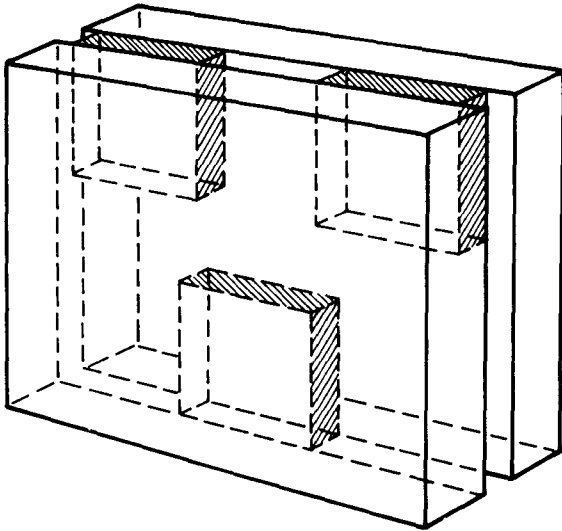


Fig. 4 Schematic diagram of the assembly in which two pieces of ceramic are separated by three spacers to form a well defined gap.

Two pieces of ceramic (5 mm deep, 3 mm wide and 50 mm high) are separated at the top by two pieces of 50  $\mu\text{m}$  thick stainless steel and at the bottom by one. This yields an assembly with a gap of varying attenuation which is extended in two dimensions (front to back and top to bottom) but only 50  $\mu\text{m}$  wide.

Using data from 64 angles, a three-dimensional reconstruction of a portion of the assembly was performed. The reconstruction volume extended 10.2 mm in x and y and 2.6 mm in z. The result is displayed in Fig. 5. Of the 91 horizontal planes reconstructed, planes 1, 46 and 91 are shown. In all slices the external shape of the specimen is well delineated. The 50  $\mu\text{m}$  steel spacers are clearly visible in slices 1 and 91. The 50  $\mu\text{m}$  gap is also visible in all the slices.

Resolution effects cause both the gap and the spacers to appear wider than they are. The three-dimensional structure of the assembly is also reproduced, with two steel spacers at the top, none in the center and one at the bottom. Note that the open areas at each spacer edge and between the top two spacers are clearly defined. These open areas represent the portion of the gap not filled by the steel spacers. In the projection images, these regions produce very little contrast and so are extremely difficult to see directly. However, the tomographic superposition of small transmission differences from many views of the specimen allows these open areas to be detected. This result is of crucial importance, since it shows that tomographic reconstruction has the potential to disclose flaws that would not be detected from a small number of views using radiography alone.

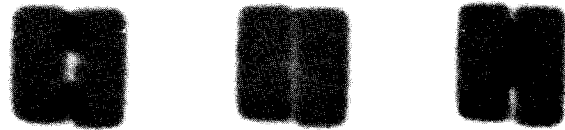


Fig. 5 Planes 1, 46 and 91 (from left to right) of the three-dimensional reconstruction of a portion of the assembly.

#### SUMMARY

We have constructed an x-ray radiographic system specifically suited to three-dimensional tomographic reconstruction. It uses video technology to image the x-ray projection of a specimen generated by a micro-focus x-ray source and fluorescent screen. A three-dimensional reconstruction algorithm is discussed and applied.

We have reconstructed the external shape of a complex object (airfoil). In addition, a ceramic assembly containing a 50  $\mu\text{m}$  gap has been reconstructed with clear detection of the 50  $\mu\text{m}$  spacers and void regions.

Current work centers on exploring the detection and reconstruction limits of the system. Improvements in the system are also contemplated. In particular, the addition of an x-ray image intensifier, other hardware, and implementation of the reconstruction algorithm on an array processor should significantly expand the system detection and reconstruction capabilities. Three-dimensional display is also being explored as a tool for detection.

#### ACKNOWLEDGMENTS

Our thanks to R. Terhune and J. Shaw for their invaluable assistance with hardware analysis, system construction and software development and implementation. Consultations with A. McLean, D. Cassidy, R. Baker and W. Trela concerning ceramic materials and their properties are gratefully acknowledged. We also appreciate the assistance of R. Temple and S. Kaberline with respect to the acquisition and utilization of computer hardware. This work was supported in part by the Office of Naval Research under contract N-00014-78-C-0714.

#### REFERENCES

1. Nudelman, S., Roehrig, H., and Capp, M. C., "A Study of Photoelectronic-Digital Radiology -- Part III: Image Acquisition Components and System Design", Proceedings of the IEEE, Vol. 70, No. 7, July 1982, pp. 715-727.
2. Herman, G. T., "Introduction", Image Reconstruction from Projections. The Fundamentals of Computerized Tomography, Academic Press, New York, 1980, pp. 1-19.
3. Robb, R. A. et al., "The Dynamic Spatial Reconstructor", Journal of Medical Systems, Vol. 4, No. 2, 1980, pp. 253-288; Robb, R. A. and Gilbert, B. K., private communication.
4. Herman, G. T., "Truly Three-Dimensional Reconstruction", Image Reconstruction from Projections. The Fundamentals of Computerized Tomography, Academic Press, New York, 1980, pp. 237-259.
5. Feldkamp, L. A., Davis, L. C., and Kress, J. W., "A Practical Cone-Beam Reconstruction Algorithm", to be published.